

Thin UHF Platform Insensitive RFID Tags

Mohamed Ali Ziai and John C. Batchelor

This paper is a postprint of a paper submitted to and accepted for publication in IET Microwaves, Antennas and Propagation and is subject to Institution of Engineering and Technology Copyright. The copy of record is available at IET Digital Library

Thin UHF Platform Insensitive RFID Tags

Mohamed Ali Ziai and John C. Batchelor

Electronics Department, The University of Kent, Canterbury, Kent, CT2 7NT

j.c.batchelor@kent.ac.uk

Indexing terms:

Radio Frequency Identification, RFID, thin tag, passive tag, tag antenna

Abstract:

RFID tags on thin substrates of less than 0.3% of a wavelength are presented. The tag antennas are formed of balanced lines wrapped around conducting rectangular patches and separated by a gap. The elements are above ground planes which lie entirely, or partially, beneath them. Good conjugate matches are offered to the RFID chip and read ranges close to the maximum quoted for a given system are achievable with these designs, even when attached to lossy or conducting bodies.

1.0 Introduction:

Use of passive Radio Frequency Identification (RFID) in supply chain and logistics applications is projected to increase dramatically in coming years for medium to long range object identification (0.5 to 10 m distance) [1, 2]. RFID tags consist of an antenna and a microchip directly integrated with no intermediate transmission line. These tags are attached in close proximity to various reflecting, lossy and capacitive bodies and may be contained within metal cages for transit [3]. Development of tags capable of communicating with RFID readers in environments that are complex and difficult for radio transmission is therefore necessary and optimisation of tag antennas for particular locations and objects is important. Certain materials pose challenges to passive RFID tagging, for instance: metallic objects cancel electric fields and liquids absorb electromagnetic waves. In both cases passive tag antennas may not receive sufficient power to excite the RFID chip and suffer significant degradation in performance [4-7]. Many objects requiring identification by passive RFID technology contain metal or liquid and it is undesirable to require specific tag

tuning for each mounting. Therefore, there is great interest to develop a passive RFID tag that is independent of the mounting platform as well as being uncomplicated in structure. Additionally a tag should be cheap, flexible, reliable and small in size and profile. Finally, the lack of a transmission line feed between the tag chip and the antenna means that the antenna input ports must offer a conjugate match to the tag chip impedance for efficient operation. Folded and meander-line dipoles printed on a polyester film have been widely studied, but are not suited for close attachment to metallic objects [8]. A planar inverted-F antenna (PIFA) or microstrip patch antenna is an attractive choice for tagging metallic objects [9-12], but they are usually considerably more expensive and not low profile. Several passive UHF RFID tags specifically tuned for mounting on metal have been recently described in the literature [13-15], patented [16, 17], or produced commercially.

The antenna described in this paper is designed for optimum performance on the surface of any object, regardless of whether it is conductive or has high dielectric constant or loss. The RFID ASIC used in these experiments is a passive UHF read only transponder, (EM4222 from EM Microelectronics [18]) with the parameters given in Table 1. Data is not available showing how the ASIC input impedance changes continuously across the bandwidth, however information for the two spot frequencies 869MHz and 915MHz suggests input impedance is only slowly varying. It is therefore possible to design a dual frequency tag by matching at the centre frequency between bands.

ID number	Data rate	Frequency	Input impedance
64 bit	256kbit s ⁻¹	869 MHz	128-j577Ω
64 bit	256kbit s ⁻¹	915 MHz	132-j553Ω

Table 1, EM4222 data

All tags were simulated using CST Microwave Studio and input match was optimised using the quasi-Newton optimizer embedded into the application. After optimization by simulation, designs were fabricated for practical validation. RFID ASIC input

impedance varies as a function of input power and in practice some physical tuning was required to provide optimum experimental read range. This process is explained in section 2.

2.0 Durable Tag:

The first tag design is shown in Figure 1 and is intended for use on pallets and containers and similar size objects where the visibility and surface area of the tag is not of primary concern. The tag, which offers some robustness to mechanical shock, is fabricated on an FR-4 substrate which separates a symmetrical resonant open dipole with 90 degree bends (elements 1, 2 and 4) from a ground plane. The design process for a 869-915MHz tag on a 3.4mm thick FR-4 substrate ($\epsilon_r = 4.9$, $\tan \delta = 0.025$) is set out below.

1. Set the width of elements 1, 2 and 4 (Fig.1) to be approximately 3% of the design wavelength (10mm). Simulation indicates this width offers a relatively wide matched band without affecting centre frequency when in close proximity to a conducting ground plane.
2. Initially set the combined length of elements 1 and 2 and 4 to be fractionally greater than a half wavelength (180mm). Introduce element 3 a few millimetres away as indicated in Fig.1 and adjust dimensions until the total length of S1 and S2 is a half wavelength at the centre frequency between 869 and 915MHz.
3. Simulation of these elements on the chosen substrate allows loading effects to be accounted for. The length and width of element 3 is used to fine tune the antenna in frequency.
4. The return loss is generally improved if the length/width ratio of element 3 is greater than 2.5.

5. The widths of slots 1 and 2 depend on the chosen substrate type and thickness and are altered by simulation to obtain the required match.
6. The input impedance of RFID ASICs varies with device and is a function of received reader power. It was therefore necessary in practice to carry out some systematic physical tuning. This was done by fabricating the simulated design and trimming the feed line width W_2 (Fig.1) to maximise read range.
7. The design was re-simulated with the new W_2 dimension and a second prototype fabricated.
8. Finally, the new prototype was tuned by trimming dimension W_a (Fig.1).

The tuned design of Table 2 was used to establish the maximum measureable reliable read range when attached to the surface of materials with differing electrical characteristics. A 500mW ERP, circularly polarised reader manufactured by Ipico [19] with optimum read range of 3 metres was used for the read range measurements which are given in Table 3. Ranges of more than 2m were measured on all surfaces.

2.1 Durable Tag on different mounting platforms:

CST MW studio was used to simulate the tag response for the laboratory environment and anechoic chamber in the three situations mentioned here: (i) in isolation, (ii) on a large metallic sheet (300mm×300mm), and (iii) on a water filled container (320×320×120mm water: $\epsilon_r = 81$, $\tan\delta = 0.01S/m$; surrounded by a 3mm thick polyimide container: $\epsilon_r = 3.5$, $\tan\delta = 0.003S/m$). The tag structure was simulated in the time domain for the entire frequency range of 0.5 – 3 GHz. A Gaussian input pulse was used and the global mesh was refined to a maximum delta convergence criterion of 0.03. The simulation results are shown in Table 4. In all cases the simulated resonance frequency remained within 1% of the frequency for the tag in isolation. This indicates negligible loading is caused by the rear structure.

In this case the substrate and ground plane extended 8mm (0.23λ) beyond the edges of the tag.

parameter	3.4mm FR4 Design		0.8mm FR4 Design		0.4mm flexible Mylar Design	
	Value (mm)	Electrical Length (λ^{-1})	Value (mm)	Electrical Length (λ^{-1})	Value (mm)	Electrical Length (λ^{-1})
L_a	104	0.301	101	0.293	115	0.333
W_a	48	0.139	40	0.116	42	0.122
W_1	10	0.029	8	0.023	5	0.014
W_2	7.5	0.022	3	0.009	2	0.006
S_1	0.32	0.0009	1	0.003	1	0.003
S_2	0.46	0.0013	1	0.003	0.3	0.0009
S_3	1	0.003	1	0.003	1	0.003
S_4	1	0.003	0	0.000	-	-
L_s	120	0.348	109	0.316	125	0.362
W_s	58	0.168	49	0.142	52	0.151
T_s	3.4	0.01	0.8	0.0023	0.4	0.001
Y	-	-	-	-	9	0.026
L_{pg}	-	-	-	-	115	0.333
W_{pg}	-	-	-	-	34	0.099

Table 2. Tag design parameters on 3.4mm and 0.8mm FR4 and 0.4mm Mylar substrates.

Tag substrate	Measurement situation	Percentage of maximum Read Range (3m)		
		In isolation	On large metallic plate	On water container
3.4mm FR4	Anechoic chamber	100%	87%	80%
	Laboratory	100%	93%	83%
0.8mm FR4	Laboratory	50%	43%	37%
400 μ m Mylar	Laboratory	50%	40%	37%

Table 3, Measured tag read range in laboratory environment and anechoic chamber in isolation, on a large metallic sheet (300mm×300mm), and on water filled container (600×400×500mm plastic container with 3mm thick walls).

The above simulations were carried out a second time with the substrate and ground plane dimensions reduced to those of the tag (i.e. $L_S=104\text{mm}$ and $W_S=48\text{mm}$). The simulated results are given in Table 4 and 5 and show that even with a truncated ground plane the resonant frequency changes by only 1.1% when attached to a large metallic object. In practice the tag with the truncated ground plane was measured to have a read range close to that of the original untruncated structure.

Table 5 gives the simulated antenna port impedance at greatest return loss for the 3 mounting conditions for the extended and truncated ground planes. In the case of the extended ground plane the impedances are observed to be insensitive to the rear mounting structures, remaining near $166+j521\Omega$ and showing good platform independence for this tag.

Substrate parameters	In isolation	On metal sheet		On water container	
	Resonant frequency (GHz)	Resonant Frequency (GHz)	Frequency change (%)	Resonant frequency (GHz)	Frequency change (%)
$L_S=120\text{mm}$, $W_S=58\text{mm}$	0.873	0.873	0.0	0.874	0.1
$L_S=104\text{mm}$, $W_S=48\text{mm}$	0.872	0.882	1.1	0.870	-0.23

Table 4: Simulated matched frequencies for 3.4mm FR4 tag in anechoic conditions (i) in isolation, (ii) on a large metallic sheet (320mm×320mm), and (iii) on a water filled container (320×320×120mm with 3mm thick polyimide walls). Percentage values

indicate loaded frequency shift when mounted on metal sheet and on water container.

Antenna port impedance (Ω)	$L_s=120, W_s=58$ (mm)	$L_s=104, W_s=48$ (mm)
In isolation	166+j521	155+j551
On large metallic plate	141+j500	85+j445
On large water bucket	148+j495	215+j583

Table 5: Simulated impedances for a tags with extended and truncated ground planes in anechoic conditions (i) in isolation, (ii) on a large metallic sheet (320mm×320mm), and (iii) on a water filled container (320×320×120mm with 3mm thick polyimide walls).

2.2 Parametric Design Study:

To appreciate the operation and design of the tag, a parametric study was carried out where the gap width between the tag elements 1, 2 and 4 and the parasitically coupled patch element 3 was altered. Figure 2 shows the impedance variation that occurs as the patch element 3 is reduced in size as S_2 is widened where $S_2=S_1+0.014$ mm. The tag is inductive for narrow gap widths with a resonant (zero reactance) point when the slot width S_1 is increased 0.5 mm beyond the optimum width for input match.

Increasing the gap width beyond the resonant point causes the coupling across the slot to diminish with the tag impedance becoming capacitive. Also shown on Fig.4 is the simulated lowest return loss frequency which is relatively insensitive to gap width changing by only 13% across the entire range of 0.2 to 4mm.

2.3 Surface Currents and radiation patterns:

Figure 3 shows the surface current at the optimum slot width ($S_1=0.32$ mm, $S_2=0.46$ mm). The figure indicates that a strong electric field has developed between the dipoles elements 1, 2, 4 and element 3 with a modal current distribution.

Simulation indicated that increasing the slot size causes the antenna port impedance to be no longer inductive and the surface current magnitude reduces meaning the ASIC functions inefficiently.

The simulated far fields indicate a main lobe directivity of 4.3dBi and show that the tag has good low directivity coverage in the forward direction as shown in Figure 4.

2.4 Thin (0.8mm) platform insensitive tag on FR-4:

The tag presented in section 2 is durable, rugged and appropriate for palette and container type applications. However, much thinner designs are desirable for carton tagging. A thinner design on 0.8mm FR-4 is presented using the same geometry as shown in Fig.1 and with the principal dimensions given in Table 2 and has a design procedure similar to that of the thicker tag. The fine tuning and conjugate impedance matching between the antenna and ASIC is achieved by adjusting the slot size 1 and 2, as shown in Figure 5. The antenna port resistance increases abruptly and stabilises at a very high value, while the antenna reactance stays inductive for slot size of up to 3 mm before the port impedance becomes capacitive. The length and width of the FR-4 substrate and ground plane are not critical but to achieve a significant read range, the substrate and ground must extend beyond the antenna edges by at least 0.01λ . Measured read range results in the laboratory environment are shown in Table 3 for comparison with the thicker design. It can be seen that shorter, though still usable, ranges of a metre are obtained for the thinner design.

The tag designs are both planar and there are no cross connections between the antenna and ground plane.

3.0 Ultra thin multilayered tag design on 350 micron Polyester substrate

Figure 6 shows the structure of a platform independent tag antenna on a flexible composite substrate formed of 2 sheets of Mylar 50 and 350 microns thick respectively. Mylar (polyimide) [20] has a relative permittivity ϵ_r equal to 2.8. The tag elements are etched into copper cladding on the upper surface of the 50 micron

layer. The structure is similar to that described in Section 2 but now also includes element 5, a parasitic patch mounted between the two substrate layers, Fig.6.

The design process for the antenna elements 1-4 with slots S1 and 2 is essentially that of the previous tag (section 2) and is carried out by simulation on the Mylar substrate with element 5 not present. The simulated curves in Fig.7 show that small slot size S2, is important in matching the tag to the ASIC though it does not significantly affect resonant frequency. After the antenna elements 1-4 have been found by simulation according to the method of section 2, the process below is then followed:

1. The parasitic plate (element 5) of length L_a and width W_{pg} is inserted into the substrate between the ground and antenna such that dimension Y is defined as indicated in Fig.6.
2. Y is varied by simulation to determine the best match to the ASIC at the centre frequency between 869 and 915MHz. Figs. 8 and 9 indicate the simulated trend of resonant frequency and tag input impedance as Y varies and show that a value between 9-22mm is required.
3. The tag is then fabricated and systematic physical tuning to maximise read range is carried out by trimming W2 as indicated in Fig.1.
4. Finally Y is varied physically to establish the longest read range.

After following the simulated and physical tuning process, the design dimensions given in Table 2 are obtained. Simulations indicated that the ultra thin tag matched frequency changed by significantly less than 1 percent when mounted in isolation, on a metal sheet or a large plastic sided water container which compares very favourably with the deviations reported for the rugged design in section 2. When fabricated for experimental validation the tag gave measured read ranges comparable with the 0.8mm FR-4 design of section 2.4 when mounted on similar backings. These ranges are given in Table 3 and indicate that a flexible ultra-thin tag with a profile of less than 0.5mm is able to exhibit a significant degree of independence from its mounting platform.

Conclusions:

This paper has introduced three designs of RFID tag antennas, in section 2, the first two were mounted on rugged FR-4 substrate and in section 3 a final design was printed on thin flexible polyester. All tags work with minimal loading effects when mounted directly on metal or absorbing platforms such as metal cans or liquid filled containers with the ultra thin Mylar tag design deviating by a small fraction of 1% when mounted on the different platforms. Ultra thin tags can be used in many applications, for example, labelling commercial goods and medical identification. All the described tag designs are planar and have no via connections though the substrate. The tag could be attached to a package as a label or printed on either face of a cardboard box.

The designs described here have been filed as patent: P40909GB.

References

1. WANT, R.: 'An Introduction to RFID Technology'. *IEEE Pervasive Computing*, 2006, **5**, (1), pp. 25-33
2. RAO, K.V.S., Nikitin, P.V. and LAM, S.F.: 'Antenna design for UHF RFID tags: a review and a practical application'. *IEEE Trans.*, 2005. **AP-53**, (12), pp. 3870-3876
3. Diugwu, C.A., Batchelor, J.C. and Fogg, M.: 'Field distributions and RFID reading within metallic roll cages'. *Electron. Letts.*, 2006, **42** (23), pp. 1326-1327
4. GRIFFIN, J.D., DURGIN, G.D., HALDI, A. and KIPPELEN, B.: 'RF Tag Antenna Performance on Various Materials Using Radio Link Budgets', *IEEE Antennas and Propagation Letters*, 2006, **5**, (1), pp. 247-250
5. DOBKIN, D. and WEIGAND, S.: 'Environmental Effects on RFID Tag Antennas', Proc. IEEE MTT-S Symposium, 2005
6. RAMAKRISHNAN, K.N.M. and DEAVOURS, D. D.: 'Performance Benchmarks for Passive UHF RFID Tags', Proc. 13th GI/ITG Conference on Measurement, Modelling and Evaluation of Computer and Communication Systems, 2006

7. AROOR, S.R. and DEAVOURS, D.D.: 'Evaluation of the State of Passive UHF RFID: An Experimental Approach', *IEEE Systems Journal*, 2007, **1** (2), pp. 168-176
8. CHOI, W., HAE WON SON, BAE, J.-H., GIL YOUNG CHOI, CHEOL SIG PYO, CHAE, J.-S.: 'An RFID Tag Using a Planar Inverted-F Antenna Capable of Being Stuck to Metallic Objects', *ETRI Journal*, 2006, **28** (2), pp. 216-218
9. HIRVONEN, M., PURSULA, P., JAAKKOLA, K. and LAUKKANEN, K.: 'Planar inverted-F antenna for radio frequency identification', *Electron. Letts.*, 2004, **40**, (14), pp. 848-850
10. UKKONEN, L., SYDANHEIRNO, L. and KIVIKOSKI, M.: 'A novel tag design using inverted-F antenna for radio frequency identification of metallic objects', Proc. IEEE/Sarnoff Symposium on Advances in Wired and Wireless Communication, 2004, pp.91 - 94
11. KWON, H. and LEE, B.: 'Compact slotted planar inverted-F RFID tag mountable on metallic objects', *Electron. Letts.*, 2005, **41**, (24), pp. 1308-1310
12. UKKONEN, L., SCHAFFRATH, M., ENGELS, D.W., SYDANHEIMO, L. and KIVIKOSKI, M.: 'Operability of Folded Microstrip Patch-Type Tag Antenna in the UHF RFID Bands within 865–928 MHz', *IEEE Antennas and Wireless Propagation Letters*, 2006, **5**, (1), pp. 414 - 417
13. CHO, C., CHOO, H.; PARK, I.: 'Design of planar RFID tag antenna for metallic objects', *Electron. Letts.*, 2008, **44** (3), pp. 175 - 177
14. RAO, K.V.S., LAM, S.F. and NIKITIN, P.V.: 'Wideband metal mount UHF RFID tag', Proc. Antennas and Propagation Society International Symposium, **AP-S**, 2008
15. SON, H.W.: 'Design of RFID tag antenna for metallic surfaces using lossy substrate', *Electron. Letts.*, 2008, **44**, (12), p. 711 - 713
16. HAUSLADEN, M.C., NASH, T.P., MITCHELL, N. and DUFFY, J.T.: 'RFID composite for mounting on metal objects', *US Pat. 6486783*, September 2000
17. FORSTER, I.J., FARR, A.N., HOWARD, N.A. and HOLMAN, A.W.: 'RFID tag using a surface insensitive antenna structure', *US Pat. 6914562*, October 2005
18. <http://www.emmicroelectronic.com/> accessed March 2009

19. <http://www.ipico.com/> accessed March 2009
20. <http://www.gts-flexible.co.uk> accessed March 2009

List of Figures:

Figure 1. Schematics of platform independent UHF passive RFID tag

Figure 2. Simulated effect of slot size variation on antenna port impedance and resonant frequency, solid line = resonant frequency (MHz), broken line = input resistance (Ohm), dotted line = input reactance (Ohm).

Figure 3. Simulated tag surface current at conjugate matched impedance ($S_1=0.32\text{mm}$, $S_2=0.46\text{mm}$).

Figure 4. H-plane tag directivity in anechoic conditions (i) short dash line: tag in isolation, (ii) long dash line: tag on a large metallic sheet ($320\text{mm}\times 320\text{mm}$), and (iii) unbroken line: tag on a water filled container ($320\times 320\times 120\text{mm}$ with 3mm thick polyimide walls).

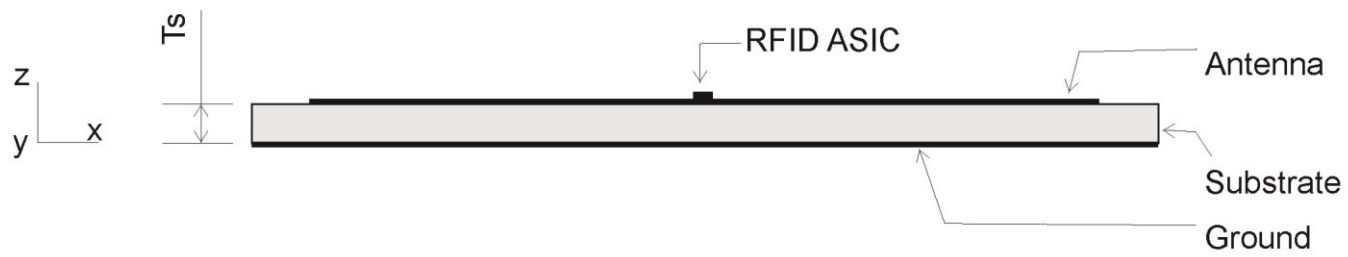
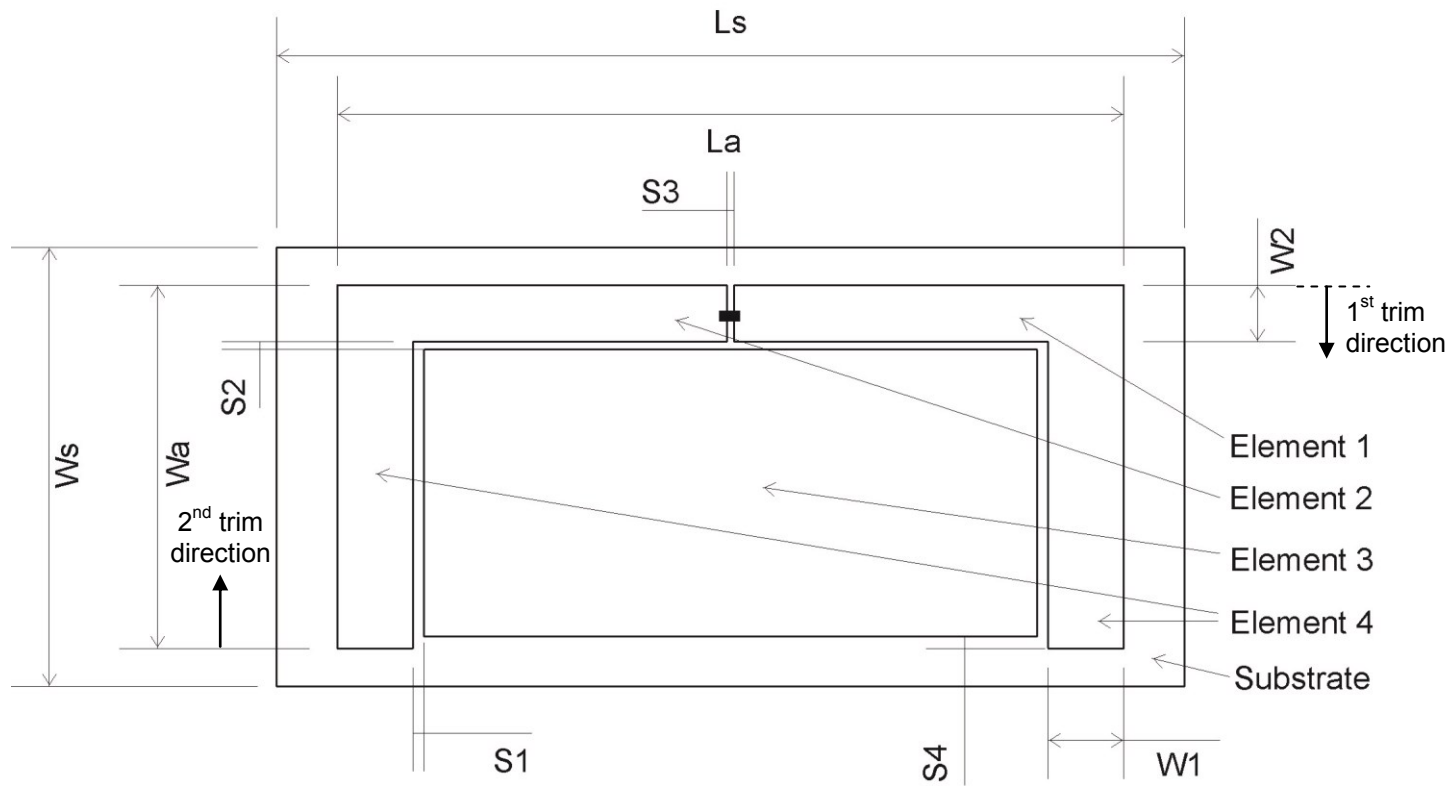
Figure 5. Simulated effect of slot size S_2 variation ($S_2=S_1+0.014\text{mm}$) on tag antenna impedance, dot-dash line = resistance (Ohm), dotted line = reactance (Ohm).

Figure 6. Schematic of flexible ultra thin tag.

Figure 7. Simulated effect of parasitic layer position Y on antenna impedance and resonant frequency, solid line = resonant frequency (MHz), broken line = input resistance (Ohm), dotted line = input reactance (Ohm).

Figure 8. Simulated effect of slot size S_2 on antenna port impedance and resonant frequency, solid line = resonant frequency (MHz), dotted line = input resistance (Ohm), broken line = input reactance (Ohm).

Figure 9. Simulated effect of parasitic layer position Y on antenna resonance frequency.



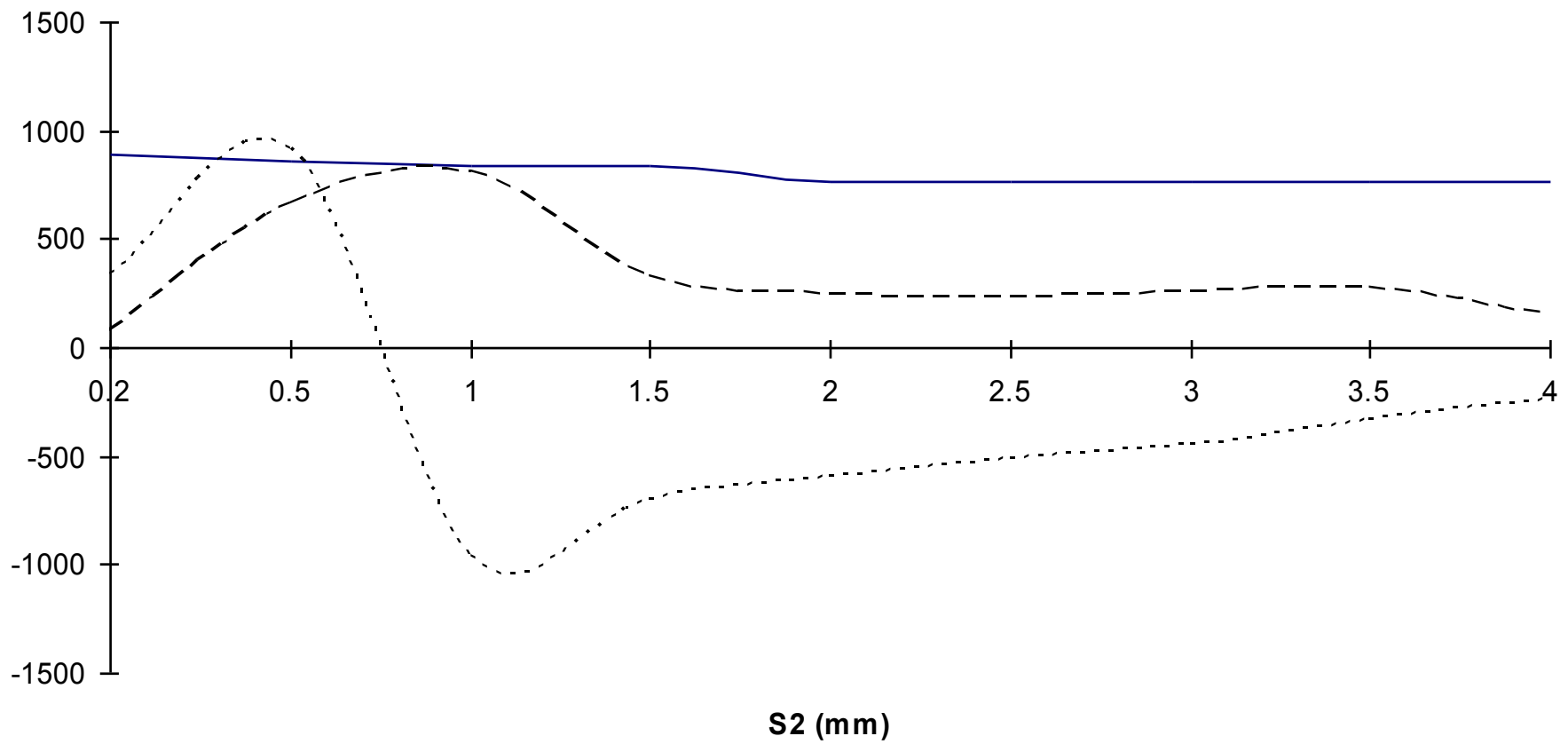


Figure 2.

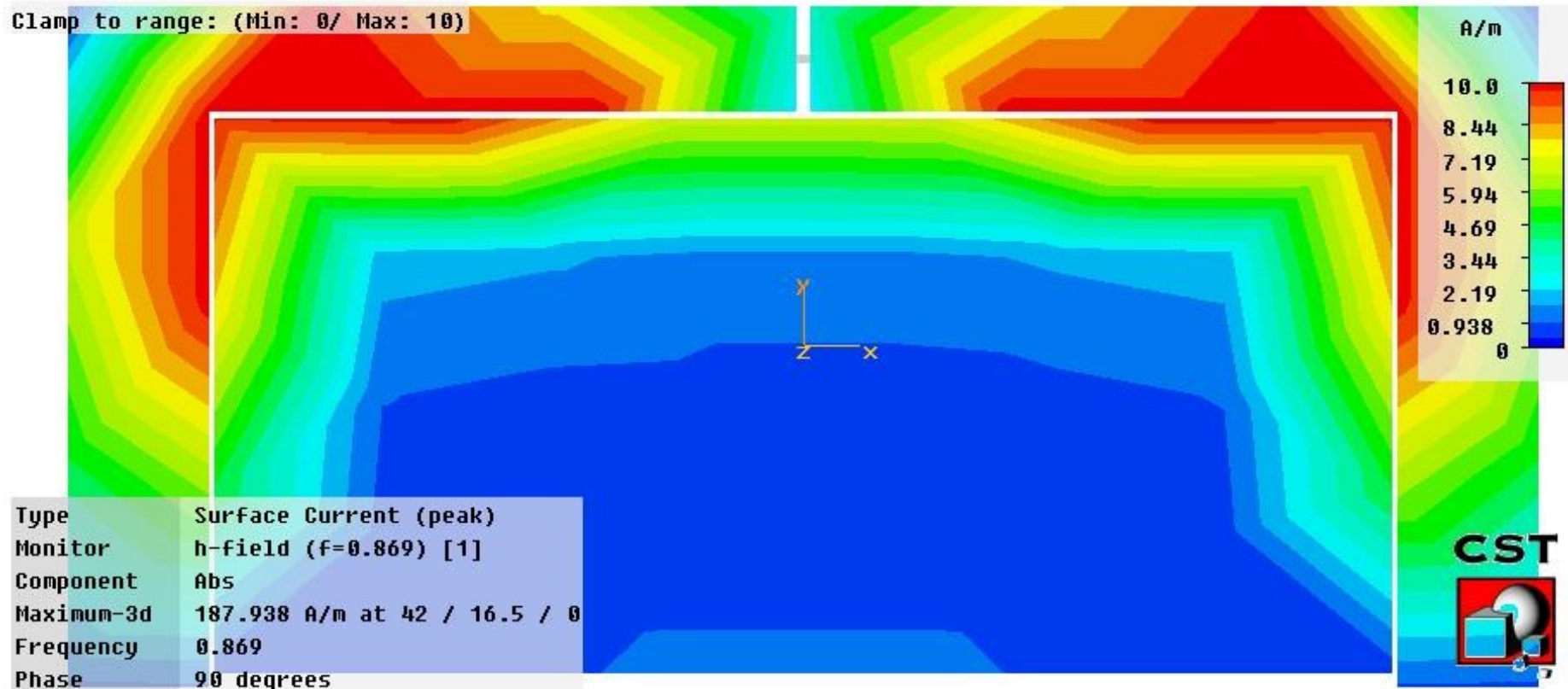


Figure 3.

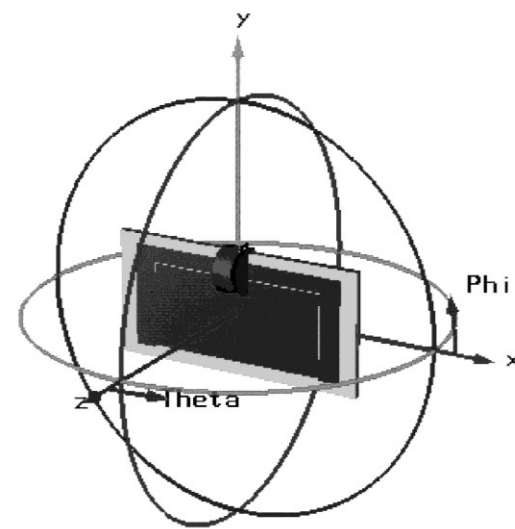
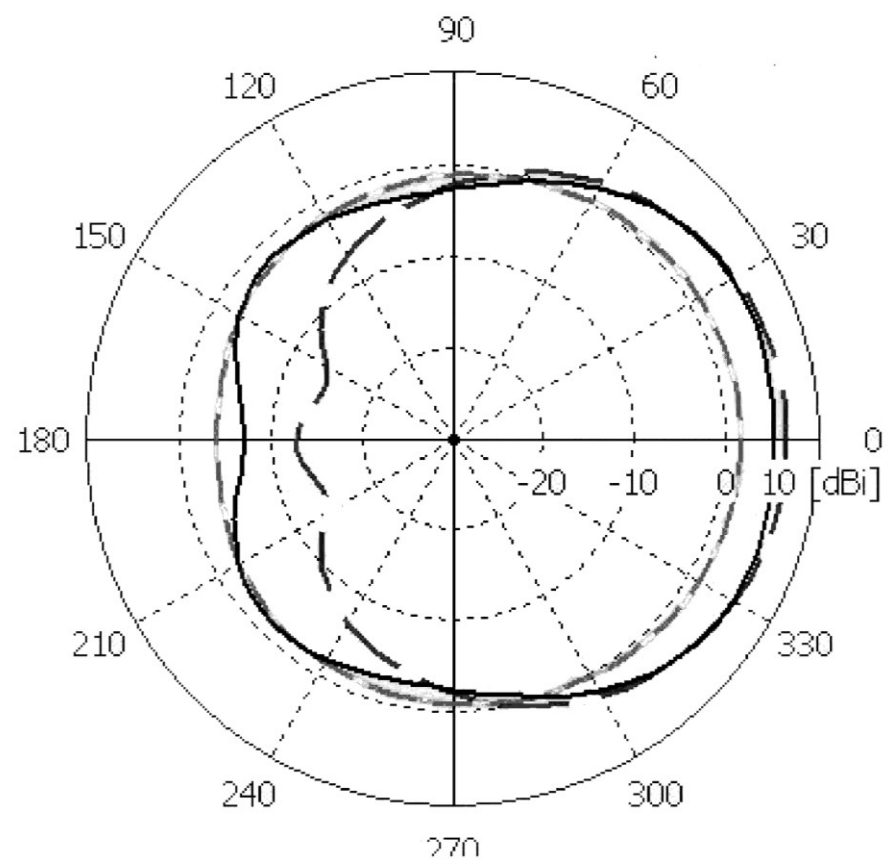


Figure 4.

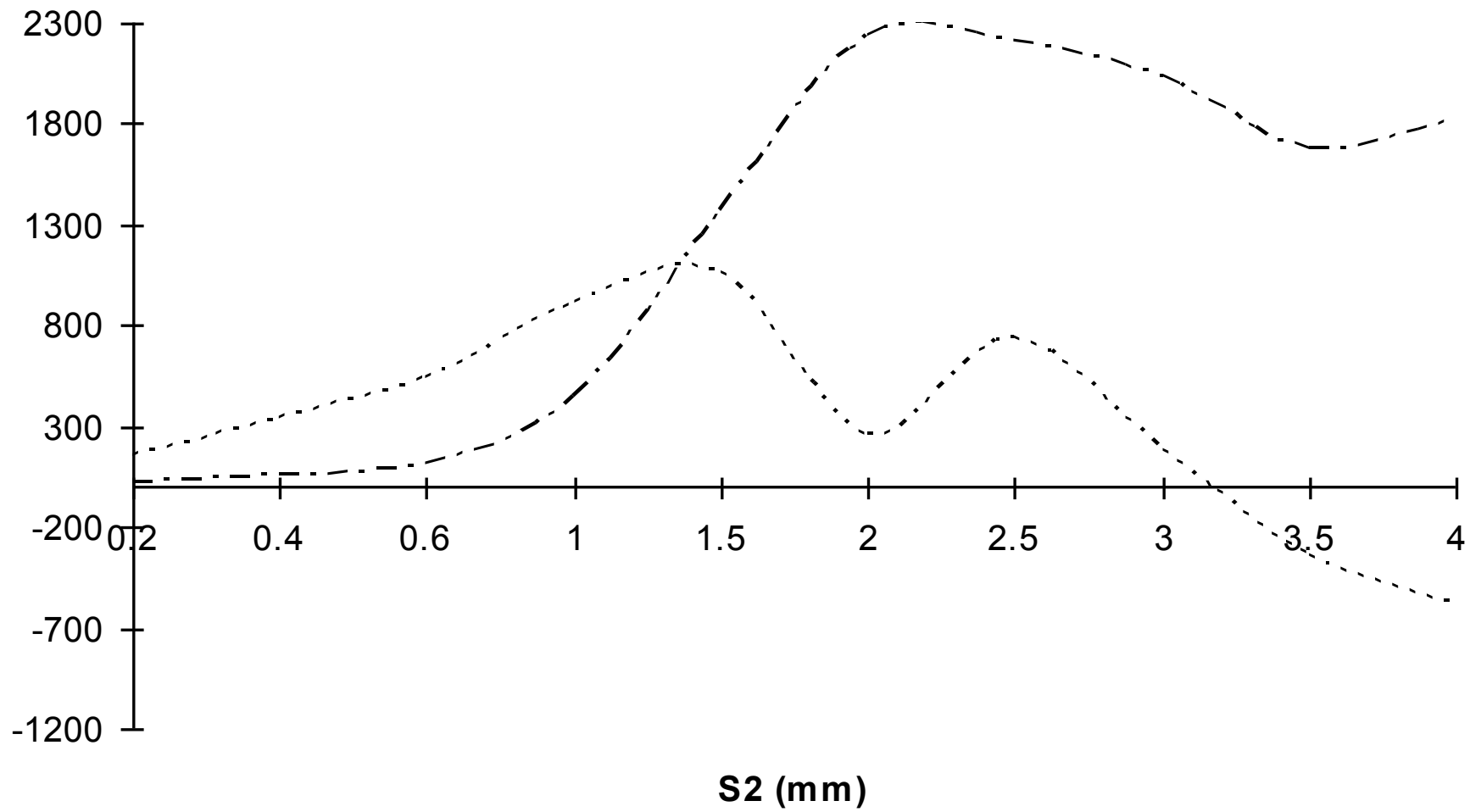


Figure 5.

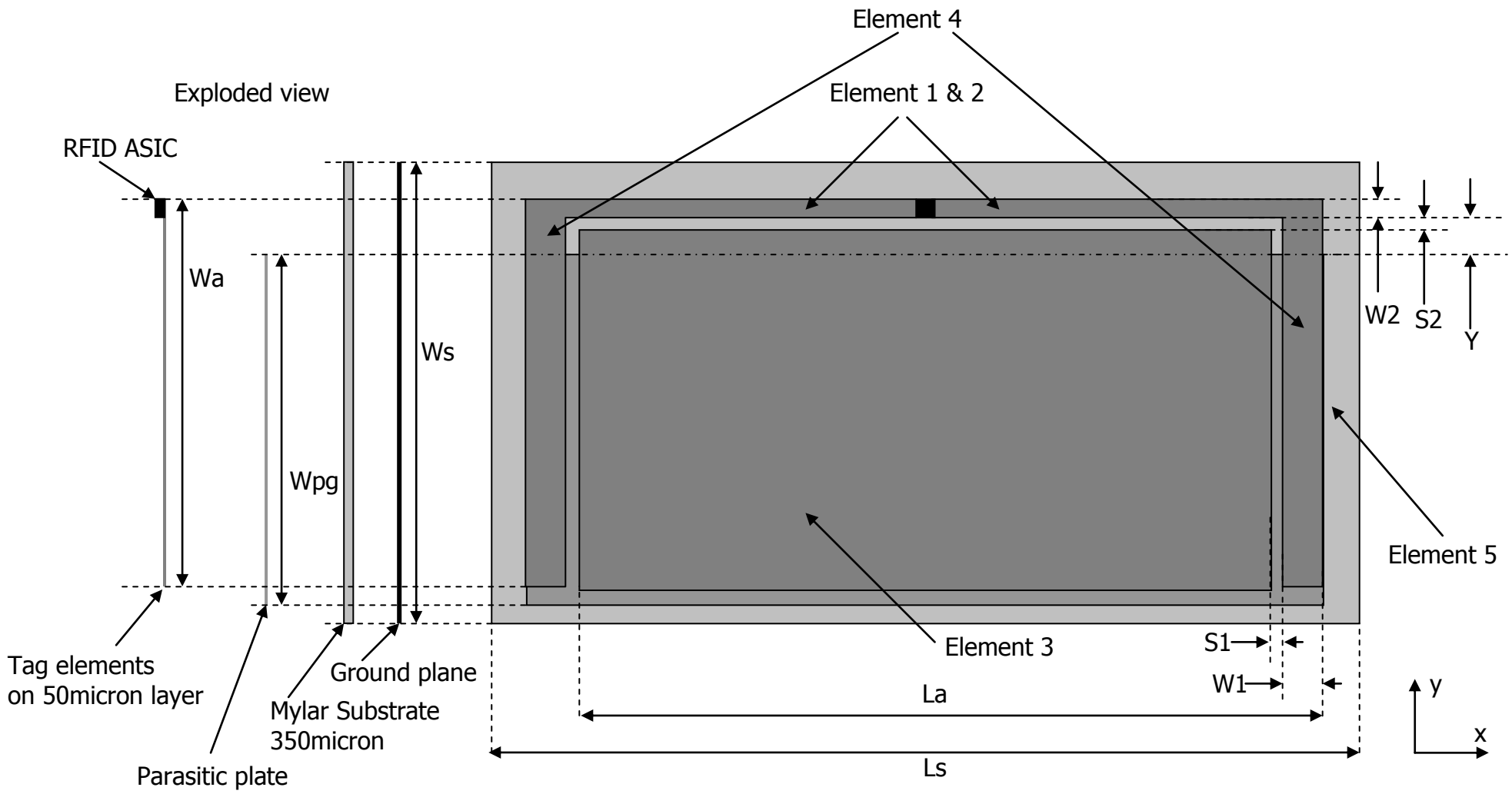


Figure 6.

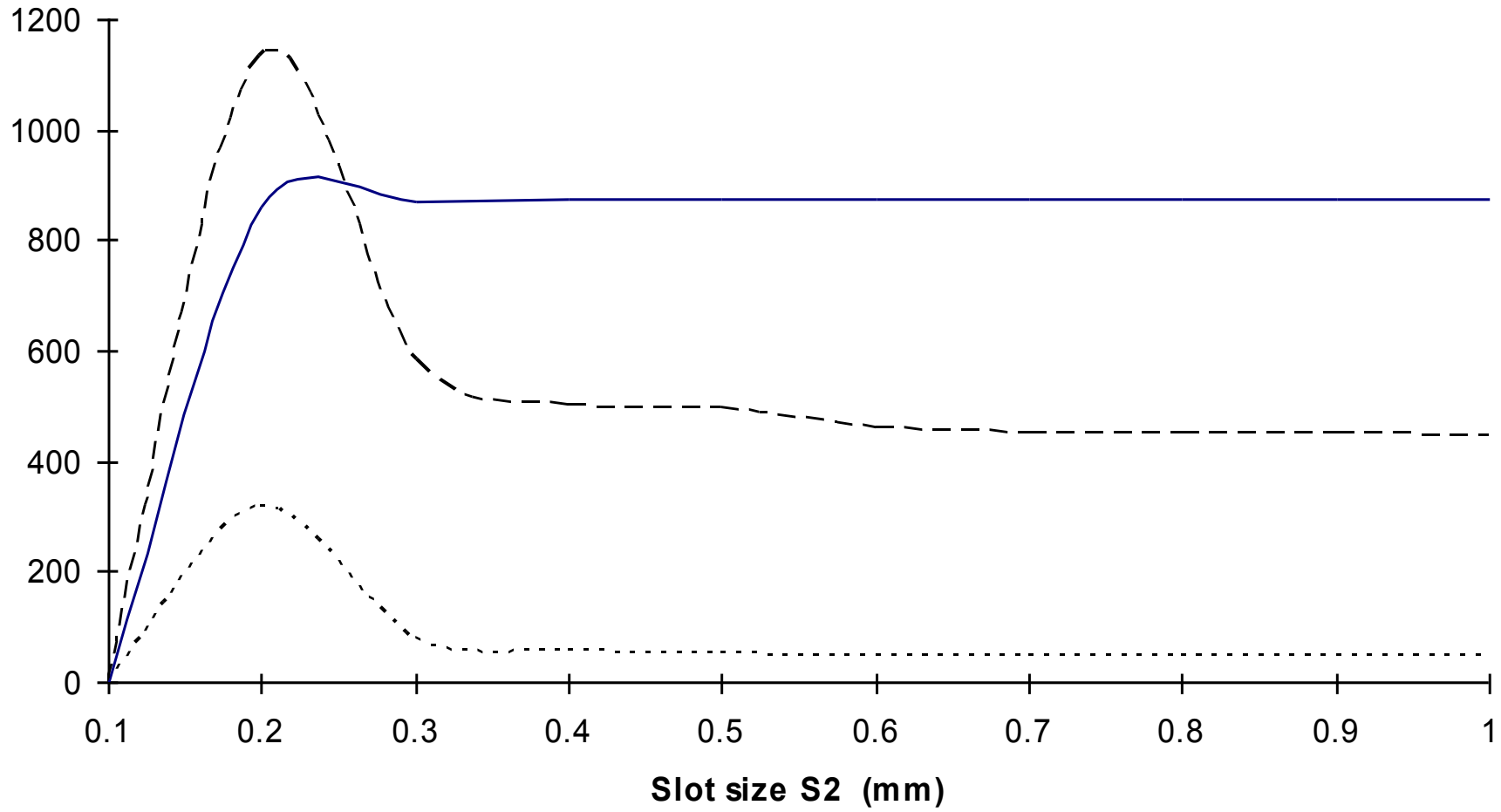


Figure 7.

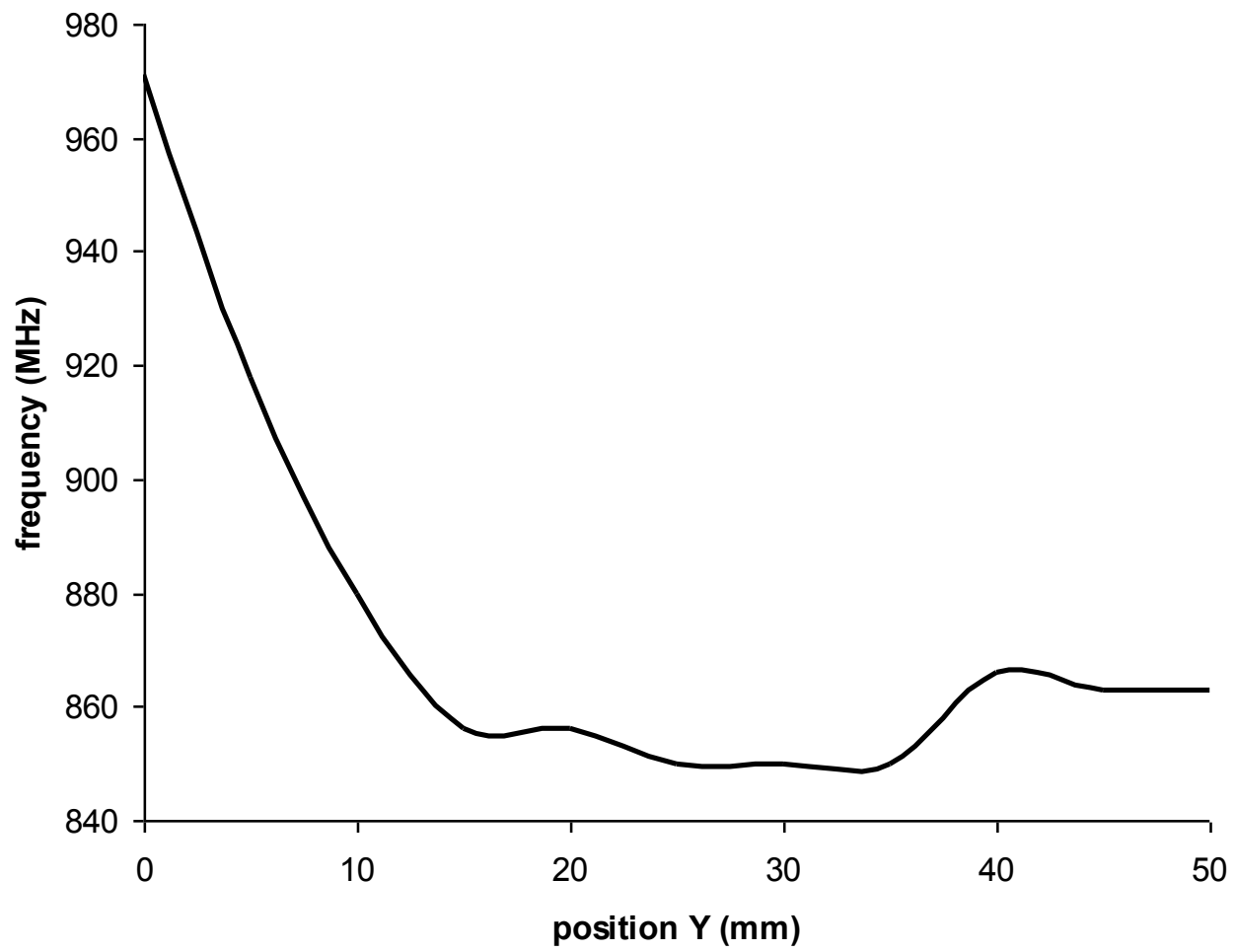


Figure 8.

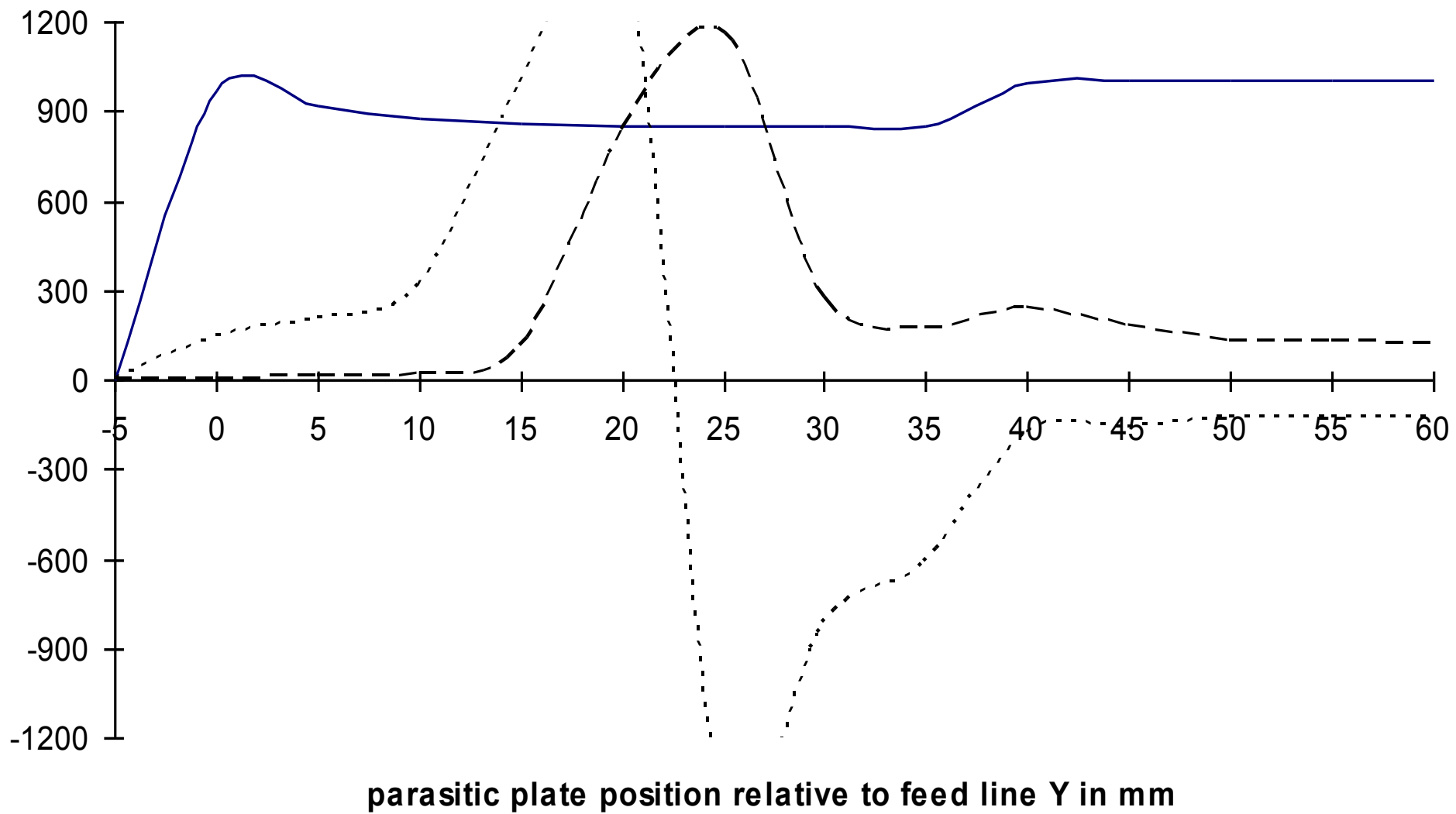


Figure 9.